

Electronic structure of wurtzite quantum dots with cylindrical symmetry

L. C. Lew Yan Voon*

*Department of Physics, Wright State University,
3640 Colonel Glenn Highway, Dayton, Ohio 45435, USA*

C. Galeriu

*Department of Physics, Worcester Polytechnic Institute,
100 Institute Road, Worcester, Massachusetts 01609, USA*

B. Lassen, M. Willatzen, and R. Melnik

*Mads Clausen Institute, University of Southern Denmark,
Grundtvigs Allé 150, DK-6400 Sønderborg, Denmark*

(Dated: October 21, 2018)

Abstract

This paper presents a six-band $\mathbf{k} \cdot \mathbf{p}$ theory for wurtzite semiconductor nanostructures with cylindrical symmetry. Our work extends the formulation of Vahala and Sercel [*Physical Review Letters* **65**, 239 (1990)] to the Rashba-Sheka-Pikus Hamiltonian for wurtzite semiconductors, without the need for the axial approximation. Results comparing our formulation for studying the electronic structure of wurtzite quantum dots with the conventional formulation are given.

I. INTRODUCTION

The III-V nitride semiconductors, with wurtzite (WZ) crystal structure, have received a great deal of attention in recent years. In the 1950's there were numerous optical studies of bulk WZ semiconductors (see Ref. 1 for a recent review). However, the detailed band structure of these materials was not studied until the discovery (in 1993) of blue light emission of WZ GaN on sapphire.² Currently the interest in WZ materials has shifted to nanostructures such as CdSe quantum rods,^{3,4,5} ZnS nanowires,⁶ ZnO nanorods⁷ and nanowires,⁸ AlN nanorods⁹ and GaN nanowires.¹⁰ On the theory side, the $\mathbf{k} \cdot \mathbf{p}$ theory of WZ bulk materials was developed by Rashba and Pikus^{11,12} and later applied to heterostructures by a number of authors.^{13,14} Mireles and Ulloa¹⁵ have applied the theory to heterostructures using the envelope function formalism of Burt¹⁶ and Foreman.¹⁷ As far as we are aware, the model has only been applied to quantum wells¹⁸ and pyramidal quantum dots.¹⁹ In 1990, Sercel and Vahala (SV) presented a new formulation of the multiband envelope function theory and applied it to spherical quantum dots and cylindrical quantum wires of zincblende (ZB) materials.^{20,21} For ZB, the SV formulation was only possible provided the axial approximation ($\gamma_2 = \gamma_3$) was made in the Hamiltonian. The theory, within the Luttinger-Kohn (LK) framework, has subsequently been applied to model quantum rods,⁵ quantum rings,²² and quantum dots.²³

The current interest in WZ nanowires²⁴ motivates the need for a model similar to the one introduced by Sercel and Vahala for ZB, for increasing the physical understanding of the $\mathbf{k} \cdot \mathbf{p}$ theory and for improving the efficiency of numerical computations for device applications. In this Letter, we propose a formulation of the Rashba-Sheka-Pikus Hamiltonian with cylindrical symmetry. We have reformulated the $\mathbf{k} \cdot \mathbf{p}$ Hamiltonian in terms of the Sercel-Vahala (SV) representation for problems with axial symmetry. The SV representation is useful because it reduces the 3D problem to a 2D one when cylindrical polar coordinates are used. Contrary to the work of Sercel and Vahala, where the axial approximation had to be introduced for ZB materials, we show that the formulation is exact for WZ materials, i.e., *no axial approximation* was needed. In addition to the fundamental interest in the SV representation of the WZ Hamiltonian, the latter also helps make for more efficient computation for problems with axial symmetry. This includes free-standing and embedded cylindrical nanowires, modulated nanowires, quantum rods, spheroidal and spherical quantum dots.

II. HAMILTONIAN

The six-band Hamiltonian for a WZ semiconductor heterostructure, in the $|X \uparrow\rangle, |Y \uparrow\rangle, |Z \uparrow\rangle, |X \downarrow\rangle, |Y \downarrow\rangle, |Z \downarrow\rangle$ basis states of the Kane model is^{12,14,15,25}

$$\widehat{H} = \frac{\hbar^2}{2m_0} \begin{pmatrix} H_k & 0 \\ 0 & H_k \end{pmatrix} + H_\Delta, \quad (1)$$

where¹⁵

$$H_k = \begin{pmatrix} \widehat{k}_x L_1 \widehat{k}_x + \widehat{k}_y M_1 \widehat{k}_y + \widehat{k}_z M_2 \widehat{k}_z & \widehat{k}_x N_1 \widehat{k}_y + \widehat{k}_y N'_1 \widehat{k}_x & \widehat{k}_x N_2 \widehat{k}_z + \widehat{k}_z N'_2 \widehat{k}_x \\ \widehat{k}_y N_1 \widehat{k}_x + \widehat{k}_x N'_1 \widehat{k}_y & \widehat{k}_x M_1 \widehat{k}_x + \widehat{k}_y L_1 \widehat{k}_y + \widehat{k}_z M_2 \widehat{k}_z & \widehat{k}_y N_2 \widehat{k}_z + \widehat{k}_z N'_2 \widehat{k}_y \\ \widehat{k}_z N_2 \widehat{k}_x + \widehat{k}_x N'_2 \widehat{k}_z & \widehat{k}_z N_2 \widehat{k}_y + \widehat{k}_y N'_2 \widehat{k}_z & \widehat{k}_x M_3 \widehat{k}_x + \widehat{k}_y M_3 \widehat{k}_y + \widehat{k}_z L_2 \widehat{k}_z \end{pmatrix}, \quad (2)$$

$$H_\Delta = \begin{pmatrix} |X \uparrow\rangle & |Y \uparrow\rangle & |Z \uparrow\rangle & |X \downarrow\rangle & |Y \downarrow\rangle & |Z \downarrow\rangle \\ \Delta_1 & -i\Delta_2 & 0 & 0 & 0 & \Delta_3 \\ i\Delta_2 & \Delta_1 & 0 & 0 & 0 & -i\Delta_3 \\ 0 & 0 & 0 & -\Delta_3 & i\Delta_3 & 0 \\ 0 & 0 & -\Delta_3 & \Delta_1 & i\Delta_2 & 0 \\ 0 & 0 & -i\Delta_3 & -i\Delta_2 & \Delta_1 & 0 \\ \Delta_3 & i\Delta_3 & 0 & 0 & 0 & 0 \end{pmatrix}. \quad (3)$$

The L_i 's, M_i 's, N_i 's and N'_i 's are the Burt-Foreman valence-band $k \cdot p$ parameters introduced by Mireles and Ulloa¹⁵; the Δ_i 's are spin-orbit parameters.¹⁵ Next, one can use the $|u_1\rangle, |u_2\rangle, |u_3\rangle, |u_4\rangle, |u_5\rangle, |u_6\rangle$ basis states defined in Ref.14. The advantage of using this basis is that now the zone-center Bloch functions are described by an angular momentum J . The envelope part of the total wave function behaves like the spherical harmonics, with an angular momentum L . The periodic Bloch space and the slowly varying envelope space are coupled by the $\mathbf{k} \cdot \mathbf{p}$ interaction. For problems with cylindrical symmetry, the projection of the total angular momentum $F_z = L_z + J_z$ is a good quantum number.

Next, we express the $\mathbf{k} \cdot \mathbf{p}$ Hamiltonian in terms of cylindrical polar coordinates ρ, ϕ, z . The total wave function is then written as

$$\begin{aligned} \psi(\mathbf{r}) &= \sum_i f_i(\mathbf{r}) |u_i\rangle = \sum_i g_i(\rho, z) e^{iL_z \phi} |u_i\rangle \\ &= \sum_i g_i(\rho, z) e^{i(F_z - J_z) \phi} |u_i\rangle = \sum_i g_i(\rho, z) |u'_i\rangle. \end{aligned} \quad (4)$$

There is a double degeneracy with respect to the sign of F_z due to inversion and time-reversal symmetry. The new matrix elements are given by

$$\begin{aligned}
& \langle f_i(\mathbf{r}) | \widehat{H} | f_j(\mathbf{r}) \rangle \\
&= \langle g_i(\rho, z) | e^{-i(F_z - J_{zi})\phi} \widehat{H} e^{i(F'_z - J_{zj})\phi} | g_j(\rho, z) \rangle \\
&= \langle g_i(\rho, z) | \widehat{H}' | g_j(\rho, z) \rangle.
\end{aligned} \tag{5}$$

These matrix elements are zero unless $F_z = F'_z$.

It is found that all ϕ dependence goes away following the SV transformation, without making an axial approximation as for ZB. The validity of this result is due to the axial symmetry already found to be true for the bulk dispersion relation.¹⁴ This can also be seen from a group theoretic point of view by noting that the group of the wave vector is the same for all wave vectors in the plane perpendicular to the c axis. Finally, the WZ Hamiltonian in cylindrical coordinates is

$$\widehat{H}' = \begin{pmatrix}
|u'_1\rangle & |u'_2\rangle & |u'_3\rangle & |u'_4\rangle & |u'_5\rangle & |u'_6\rangle \\
\begin{matrix} S_{11} \\ +\Delta_1 + \Delta_2 \end{matrix} & S_{12} & S_{13} & 0 & 0 & 0 \\
S_{21} & \begin{matrix} S_{22} \\ +\Delta_1 - \Delta_2 \end{matrix} & S_{23} & 0 & 0 & \sqrt{2}\Delta_3 \\
S_{31} & S_{32} & S_{33} & 0 & \sqrt{2}\Delta_3 & 0 \\
0 & 0 & 0 & \begin{matrix} S_{44} \\ +\Delta_1 + \Delta_2 \end{matrix} & S_{45} & S_{46} \\
0 & 0 & \sqrt{2}\Delta_3 & S_{54} & \begin{matrix} S_{55} \\ +\Delta_1 - \Delta_2 \end{matrix} & S_{56} \\
0 & \sqrt{2}\Delta_3 & 0 & S_{64} & S_{65} & S_{66}
\end{pmatrix}, \tag{6}$$

where

$$\begin{aligned}
S_{11} &= -\frac{\hbar^2}{2m_0} \frac{1}{2} \left\{ \frac{\partial}{\partial \rho} \left((L_1 + M_1) \frac{\partial}{\partial \rho} \right) + \frac{(L_1 + M_1)}{\rho} \frac{\partial}{\partial \rho} \right. \\
&\quad \left. + 2 \frac{\partial}{\partial z} M_2 \frac{\partial}{\partial z} - \frac{(F_z - J_1)}{\rho} \frac{\partial (N_1 - N'_1)}{\partial \rho} - \frac{(F_z - J_1)^2}{\rho^2} (L_1 + M_1) \right\}, \\
S_{22} &= -\frac{\hbar^2}{2m_0} \frac{1}{2} \left\{ \frac{\partial}{\partial \rho} \left((L_1 + M_1) \frac{\partial}{\partial \rho} \right) + \frac{(L_1 + M_1)}{\rho} \frac{\partial}{\partial \rho} \right.
\end{aligned}$$

$$\begin{aligned}
& + 2\frac{\partial}{\partial z}M_2\frac{\partial}{\partial z} + \frac{(F_z - J_2)}{\rho}\frac{\partial(N_1 - N'_1)}{\partial\rho} - \frac{(F_z - J_2)^2}{\rho^2}(L_1 + M_1) \Big\}, \\
S_{33} &= -\frac{\hbar^2}{2m_0}\left\{\frac{\partial}{\partial\rho}\left(M_3\frac{\partial}{\partial\rho}\right) + \frac{M_3}{\rho}\frac{\partial}{\partial\rho} + \frac{\partial}{\partial z}L_2\frac{\partial}{\partial z} - \frac{(F_z - J_3)^2}{\rho^2}M_3\right\}, \\
S_{12} &= \frac{\hbar^2}{2m_0}\frac{1}{2}\left\{\frac{\partial}{\partial\rho}\left((L_1 - M_1)\frac{\partial}{\partial\rho}\right) + (F_z - J_2)\frac{\partial}{\partial\rho}\left(\frac{(L_1 - M_1)}{\rho}\right)\right. \\
& \left. + (F_z - J_2 - 1)\frac{(L_1 - M_1)}{\rho}\frac{\partial}{\partial\rho} + \frac{(F_z - J_2)(F_z - J_2 - 1)}{\rho^2}(L_1 - M_1)\right\}, \\
S_{21} &= \frac{\hbar^2}{2m_0}\frac{1}{2}\left\{\frac{\partial}{\partial\rho}\left((L_1 - M_1)\frac{\partial}{\partial\rho}\right) - (F_z - J_1)\frac{\partial}{\partial\rho}\left(\frac{(L_1 - M_1)}{\rho}\right)\right. \\
& \left. - (F_z - J_1 + 1)\frac{(L_1 - M_1)}{\rho}\frac{\partial}{\partial\rho} + \frac{(F_z - J_1)(F_z - J_1 + 1)}{\rho^2}(L_1 - M_1)\right\}, \\
S_{13} &= \frac{\hbar^2}{2m_0}\frac{1}{\sqrt{2}}\left\{\frac{\partial}{\partial\rho}\left(N_2\frac{\partial}{\partial z}\right) + \frac{\partial}{\partial z}\left(N'_2\frac{\partial}{\partial\rho}\right) + (F_z - J_3)\left[\frac{\partial}{\partial z}\left(\frac{N'_2}{\rho}\right) + \frac{N_2}{\rho}\frac{\partial}{\partial z}\right]\right\}, \\
S_{31} &= \frac{\hbar^2}{2m_0}\frac{1}{\sqrt{2}}\left\{\frac{\partial}{\partial\rho}\left(N'_2\frac{\partial}{\partial z}\right) + \frac{\partial}{\partial z}\left(N_2\frac{\partial}{\partial\rho}\right) - (F_z - J_1)\left[\frac{\partial}{\partial z}\left(\frac{N_2}{\rho}\right) + \frac{N'_2}{\rho}\frac{\partial}{\partial z}\right]\right\}, \quad (7) \\
S_{23} &= -\frac{\hbar^2}{2m_0}\frac{1}{\sqrt{2}}\left\{\frac{\partial}{\partial\rho}\left(N_2\frac{\partial}{\partial z}\right) + \frac{\partial}{\partial z}\left(N'_2\frac{\partial}{\partial\rho}\right) - (F_z - J_3)\left[\frac{\partial}{\partial z}\left(\frac{N'_2}{\rho}\right) + \frac{N_2}{\rho}\frac{\partial}{\partial z}\right]\right\}, \\
S_{32} &= -\frac{\hbar^2}{2m_0}\frac{1}{\sqrt{2}}\left\{\frac{\partial}{\partial\rho}\left(N'_2\frac{\partial}{\partial z}\right) + \frac{\partial}{\partial z}\left(N_2\frac{\partial}{\partial\rho}\right) + (F_z - J_2)\left[\frac{\partial}{\partial z}\left(\frac{N_2}{\rho}\right) + \frac{N'_2}{\rho}\frac{\partial}{\partial z}\right]\right\}, \\
S_{44} &= -\frac{\hbar^2}{2m_0}\frac{1}{2}\left\{\frac{\partial}{\partial\rho}\left((L_1 + M_1)\frac{\partial}{\partial\rho}\right) + \frac{(L_1 + M_1)}{\rho}\frac{\partial}{\partial\rho}\right. \\
& \left. + 2\frac{\partial}{\partial z}M_2\frac{\partial}{\partial z} + \frac{(F_z - J_4)}{\rho}\frac{\partial(N_1 - N'_1)}{\partial\rho} - \frac{(F_z - J_4)^2}{\rho^2}(L_1 + M_1)\right\}, \\
S_{55} &= -\frac{\hbar^2}{2m_0}\frac{1}{2}\left\{\frac{\partial}{\partial\rho}\left((L_1 + M_1)\frac{\partial}{\partial\rho}\right) + \frac{(L_1 + M_1)}{\rho}\frac{\partial}{\partial\rho}\right. \\
& \left. + 2\frac{\partial}{\partial z}M_2\frac{\partial}{\partial z} - \frac{(F_z - J_5)}{\rho}\frac{\partial(N_1 - N'_1)}{\partial\rho} - \frac{(F_z - J_5)^2}{\rho^2}(L_1 + M_1)\right\}, \\
S_{66} &= -\frac{\hbar^2}{2m_0}\left\{\frac{\partial}{\partial\rho}\left(M_3\frac{\partial}{\partial\rho}\right) + \frac{M_3}{\rho}\frac{\partial}{\partial\rho} + \frac{\partial}{\partial z}L_2\frac{\partial}{\partial z} - \frac{(F_z - J_6)^2}{\rho^2}M_3\right\}, \\
S_{45} &= \frac{\hbar^2}{2m_0}\frac{1}{2}\left\{\frac{\partial}{\partial\rho}\left((L_1 - M_1)\frac{\partial}{\partial\rho}\right) - (F_z - J_5)\frac{\partial}{\partial\rho}\left(\frac{(L_1 - M_1)}{\rho}\right)\right. \\
& \left. - (F_z - J_5 + 1)\frac{(L_1 - M_1)}{\rho}\frac{\partial}{\partial\rho} + \frac{(F_z - J_5)(F_z - J_5 + 1)}{\rho^2}(L_1 - M_1)\right\}, \\
S_{54} &= \frac{\hbar^2}{2m_0}\frac{1}{2}\left\{\frac{\partial}{\partial\rho}\left((L_1 - M_1)\frac{\partial}{\partial\rho}\right) + (F_z - J_4)\frac{\partial}{\partial\rho}\left(\frac{(L_1 - M_1)}{\rho}\right)\right. \\
& \left. + (F_z - J_4 - 1)\frac{(L_1 - M_1)}{\rho}\frac{\partial}{\partial\rho} + \frac{(F_z - J_4)(F_z - J_4 - 1)}{\rho^2}(L_1 - M_1)\right\},
\end{aligned}$$

$$\begin{aligned}
S_{46} &= -\frac{\hbar^2}{2m_0\sqrt{2}} \left\{ \frac{\partial}{\partial\rho} \left(N_2 \frac{\partial}{\partial z} \right) + \frac{\partial}{\partial z} \left(N_2' \frac{\partial}{\partial\rho} \right) - (F_z - J_6) \left[\frac{\partial}{\partial z} \left(\frac{N_2'}{\rho} \right) + \frac{N_2}{\rho} \frac{\partial}{\partial z} \right] \right\}, \\
S_{56} &= \frac{\hbar^2}{2m_0\sqrt{2}} \left\{ \frac{\partial}{\partial\rho} \left(N_2 \frac{\partial}{\partial z} \right) + \frac{\partial}{\partial z} \left(N_2' \frac{\partial}{\partial\rho} \right) + (F_z - J_6) \left[\frac{\partial}{\partial z} \left(\frac{N_2'}{\rho} \right) + \frac{N_2}{\rho} \frac{\partial}{\partial z} \right] \right\}, \\
S_{64} &= -\frac{\hbar^2}{2m_0\sqrt{2}} \left\{ \frac{\partial}{\partial\rho} \left(N_2' \frac{\partial}{\partial z} \right) + \frac{\partial}{\partial z} \left(N_2 \frac{\partial}{\partial\rho} \right) + (F_z - J_4) \left[\frac{\partial}{\partial z} \left(\frac{N_2'}{\rho} \right) + \frac{N_2}{\rho} \frac{\partial}{\partial z} \right] \right\}, \\
S_{65} &= \frac{\hbar^2}{2m_0\sqrt{2}} \left\{ \frac{\partial}{\partial\rho} \left(N_2' \frac{\partial}{\partial z} \right) + \frac{\partial}{\partial z} \left(N_2 \frac{\partial}{\partial\rho} \right) - (F_z - J_5) \left[\frac{\partial}{\partial z} \left(\frac{N_2'}{\rho} \right) + \frac{N_2}{\rho} \frac{\partial}{\partial z} \right] \right\},
\end{aligned}$$

where $J_n \equiv J_{zn}$. Note that in general $S_{ij} \neq S_{ji}^\dagger$. That the matrix representation is nonhermitian is due to the chosen representation and to the fact that the Hilbert space is now divided into F_z subspaces. An analogous result was obtained previously for the SV representation of zincblende quantum rings.²²

III. NUMERICAL RESULTS AND DISCUSSION

A free standing WZ GaN cylindrical quantum dot, with a radius of 50 Å and a height of 100 Å, with the axis along the crystallographic c -axis, has been studied using both the 3D and 2D methods. The parameters for GaN have been taken from the literature.²⁵ The 3D Hamiltonian (1) and the 2D Hamiltonian (6) have been implemented using FEMLAB; this is a software using the finite element method. Different meshes have been generated, and the convergence of the eigenvalues has been studied. Due to the reduced dimensionality, the eigenvalue problem in 2D can be solved much faster, in minutes instead of hours, and with less memory requirements than the eigenvalue problem in 3D. After only one mesh refinement (2040 elements) the 2D eigenvalues have converged. However, even after three mesh refinements (3967 elements) the 3D eigenvalues are not fully converged, as seen from Fig. 1.

A free standing WZ CdSe cylindrical quantum dot, with a radius of 50 Å and a height of 40–150 Å, has also been investigated. The parameters for CdSe have been taken from the literature.^{13,28} By varying the height we can study shape effects on semiconductor nanocrystals. From Figures 2-3 we notice that there are crossings between states with $F_z = 1/2$ (solid lines) and $F_z = 3/2$ (dotted lines). The inclusion of the linear term in the Hamiltonian dramatically changes the energy band structure, and results in anticrossings between energy bands²⁶.

In CdSe nanocrystals with a radius of 15 Å and a gelcap shape a crossing between the lowest two valence sublevels appears at an aspect ratio of 1.25.³ There are also some experimental studies of the transition from 3D to 2D confinement in CdSe quantum rods.^{3,29} Theoretical work on the electronic properties of the transition reported so far include empirical pseudopotential calculations on a rather artificial shape,³ and $\mathbf{k} \cdot \mathbf{p}$ calculations for cylindrical ZB structures^{5,30} and for spheroidal WZ structures.²⁸ We hope that our formulation for studying the electronic structure of wurzite quantum dots with cylindrical symmetry will be a very useful tool in this important research area.

IV. CONCLUSIONS

We have extended the Sercel-Vahala technique to WZ heterostructures with cylindrical symmetry and shown this to be an exact result. This is crucial for applications in enabling greatly decreased computational resources. We have studied GaN and CdSe cylindrical quantum dots, calculating the effect of the aspect ratio on energy levels and wavefunctions.

Acknowledgments

The work was supported by an NSF CAREER award (NSF Grant No. 9984059, 0454849), and by a Research Challenge grant from Wright State University and the Ohio Board of Regents.

-
- * Electronic address: lok.lewyanvoon@wright.edu
- ¹ L. C. Lew Yan Voon, M. Willatzen, M. Cardona, and N. E. Christensen, *Phys. Rev. B* **53**, 10703 (1996).
 - ² S. Nakamura, S. Pearton, and G. Fasol, *The Blue Laser Diode* (Springer, New York, 2000).
 - ³ J. Hu, L. Li, W. Yang, L. Manna, L. Wang, and A. P. Alivisatos, *Science* **292**, 2060 (2001).
 - ⁴ L. Li, J. Hu, W. Yang, and A. P. Alivisatos, *Nano Lett.* **1**, 349 (2001).
 - ⁵ D. Katz, T. Wizansky, O. Millo, E. Rothenberg, T. Mokari, and U. Banin, *Phys. Rev. Lett.* **89**, 086801 (2002).
 - ⁶ Y. Wang, L. Zhang, C. Liang, G. Wang, and X. Peng, *Chem. Phys. Lett.* **357**, 314 (2002).
 - ⁷ Z. R. Tian, J. A. Voigt, J. Liu, B. McKenzie, M. J. McDermott, M. A. Rodriguez, H. Konishi, and H. Xu, *Nature Materials* **2**, 821 (2003).
 - ⁸ M. H. Huang, S. Mao, H. Feick, H. Yan, Y. Wu, H. Kind, E. Weber, R. Russo, and P. Yang, *Science* **292**, 1897 (2001).
 - ⁹ Q. L. Liu, T. Tanaka, J. Q. Hu, F. F. Xu, and T. Sekiguchi, *Appl. Phys. Lett.* **83**, 4939 (2003).
 - ¹⁰ J. C. Johnson, H. Choi, K. P. Knutsen, R. D. Schaller, P. Yang, and R. J. Saykally, *Nature Materials* **1**, 106 (2002).
 - ¹¹ E. I. Rashba, *Sov. Phys. Solid State* **1**, 368 (1959).
 - ¹² G. L. Bir and G. E. Pikus, *Symmetry and Strain-Induced Effects in Semiconductors* (Wiley, New York, 1975).
 - ¹³ J.-B. Jeon, Y. M. Sirenko, K. W. Kim, M. A. Littlejohn, and M. A. Stroscio, *Solid State Comm.* **99**, 423 (1996).
 - ¹⁴ S. L. Chuang and C. S. Chang, *Phys. Rev. B* **54**, 2491 (1996).
 - ¹⁵ F. Mireles and S. E. Ulloa, *Phys. Rev. B* **60**, 13659 (1999).
 - ¹⁶ M. G. Burt, *J. Phys.: Condens. Matter* **4**, 6651 (1992).
 - ¹⁷ B. A. Foreman, *Phys. Rev. B* **56**, R12748 (1997).
 - ¹⁸ S. L. Chuang and C. S. Chang, *Semicond. Sci. Technol.* **12**, 252 (1997).
 - ¹⁹ A. D. Andreev and E. P. O'Reilly, *Phys. Rev. B* **62**, 15851 (2000).
 - ²⁰ K. J. Vahala and P. C. Sercel, *Phys. Rev. Lett.* **65**, 239 (1990).
 - ²¹ P. C. Sercel and K. J. Vahala, *Phys. Rev. B* **42**, 3690 (1990).

- ²² J. Planelles, W. Jaskólski, and J. I. Aliaga, *Phys. Rev. B* **65**, 033306 (2002).
- ²³ F. B. Pedersen and Y.-C. Chang, *Phys. Rev. B* **53**, 1507 (1996).
- ²⁴ X. Duan and C. M. Lieber, *Adv. Mat.* **12**, 298 (2000).
- ²⁵ V. A. Fonoberov and A. A. Balandin, *J. Appl. Phys.* **94**, 7178 (2003).
- ²⁶ J.-B. Xia, K. W. Cheah, X.-L. Wang, D.-Z. Sun, and M.-Y. Kong, *Phys. Rev. B* **59**, 10119 (1999).
- ²⁷ J.-B. Xia and J. Li, *Phys. Rev. B* **60**, 11540 (1999).
- ²⁸ X.-Z. Li and J.-B. Xia, *Phys. Rev. B* **66**, 115316 (2002).
- ²⁹ H. Yu, J. Li, R. A. Loomis, P. C. Gibbons, L.-W. Wang, and W. E. Buhro, *J. Am. Chem. Soc.* **125**, 16168 (2003).
- ³⁰ L. C. Lew Yan Voon, R. Melnik, B. Lassen, and M. Willatzen, *Nano Lett.* **4**, 289 (2004).

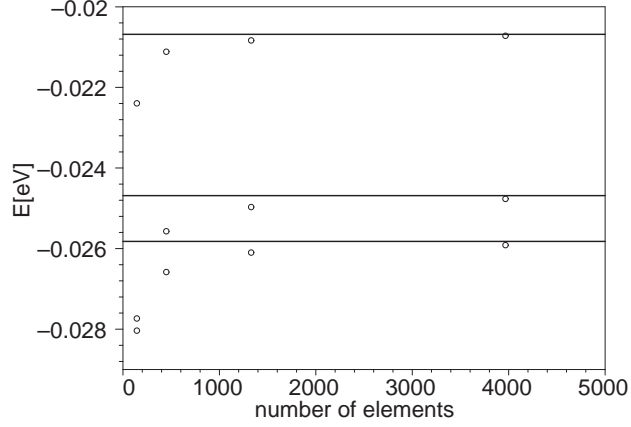


FIG. 1: The energies of the top three valence sublevels of a WZ GaN cylindrical quantum dot, calculated with the 3D program (circles). The solid lines are the converged values obtained with the 2D program.

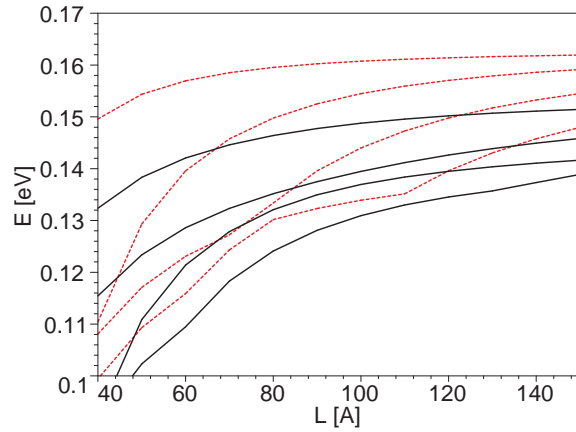


FIG. 2: The energies of the lowest states as a function of the CdSe quantum dot aspect ratio. The linear term is not included in the Hamiltonian. Shown are the first four states with $F_z = 1/2$ (solid lines) and with $F_z = 3/2$ (dotted lines).

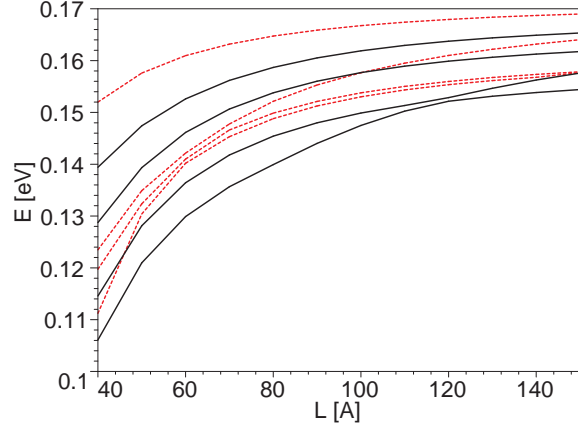


FIG. 3: The energies of the lowest states as a function of the CdSe quantum dot aspect ratio. The linear term is included in the Hamiltonian. Shown are the first four states with $F_z = 1/2$ (solid lines) and with $F_z = 3/2$ (dotted lines).